Defraeye T., Blocken B., Koninckx E., Hespel P., Verboven P., Nicolai B., Carmeliet J. (2014), Cyclist drag in team pursuit: influence of cyclist sequence, stature and arm spacing, *Journal of Biomechanical Engineering* 136 (1), 011005. http://dx.doi.org/10.1115/1.4025792
Author manuscript: the content is identical to the content of the published paper, but without the final typesetting by the publisher

Cyclist drag in team pursuit: influence of cyclist sequence, stature, and arm spacing

Thijs Defraeye [a,*], Bert Blocken [b], Erwin Koninckx [c,d], Peter Hespel [d], Pieter Verboven [a], Bart Nicolai [a], Jan Carmeliet [e,f]

[a] *MeBioS, Department of Biosystems, KU Leuven, Willem de Croylaan 42, 3001 Heverlee, Belgium*

[b] *Building Physics and Services, Eindhoven University of Technology, P.O. Box 513, 5600*

[c] *Flemish Cycling Federation, Globelaan 49/2, 1190 Brussels, Belgium*

[d] *Research Centre for Exercise Physiology, Department of Kinesiology, KU Leuven, Tervuursevest 101, 3001 Heverlee, Belgium*

[e] *Chair of Building Physics, Swiss Federal Institute of Technology Zurich (ETHZ), Wolfgang-Pauli-Strasse 15, 8093 Zürich, Switzerland*

[f] *Laboratory for Building Science and Technology, Swiss Federal Laboratories for Materials Testing and Research (Empa), Überlandstrasse 129, 8600 Dübendorf, Switzerland*

Keywords

CFD; air flow; aerodynamic interference; wake; turbulence

[*] Corresponding author. Tel.: +32 (0)16321348; Fax: +32 (0)16321980.
E-mail address: thijs.defraeye@biw.kuleuven.be

Defraeye T., Blocken B., Koninckx E., Hespel P., Verboven P., Nicolai B., Carmeliet J. (2014), Cyclist drag in team pursuit: influence of cyclist sequence, stature and arm spacing, *Journal of Biomechanical Engineering* 136 (1), 011005. http://dx.doi.org/10.1115/1.4025792
Author manuscript: the content is identical to the content of the published paper, but without the final typesetting by the publisher

Abstract

In team pursuit, the drag of a group of cyclists riding in a pace line is dependent on several factors, such as anthropometric characteristics (stature) and position of each cyclist as well as the sequence in which they ride. To increase insight in drag reduction mechanisms, the aerodynamic drag of four cyclists riding in a pace line was investigated, using four different cyclists, and for four different sequences. In addition, each sequence was evaluated for two arm spacings. Instead of conventional field or wind-tunnel experiments, a validated numerical approach (computational fluid dynamics) was used to evaluate cyclist drag, where the bicycles were not included in the model. The cyclist drag was clearly dependent on his position in the pace line, where second and subsequent positions experienced a drag reduction up to 40%, compared to an individual cyclist. Individual differences in stature and position on the bicycle led to an intercyclist variation of this drag reduction at a specific position in the sequence, but also to a variation of the total drag of the group for different sequences. A larger drag area for the group was found when riding with wider arm spacing. Such numerical studies on cyclists in a pace line are useful for determining the optimal cyclist sequence for team pursuit.

Defraeye T., Blocken B., Koninckx E., Hespel P., Verboven P., Nicolai B., Carmeliet J. (2014), Cyclist drag in team pursuit: influence of cyclist sequence, stature and arm spacing, *Journal of Biomechanical Engineering* 136 (1), 011005. http://dx.doi.org/10.1115/1.4025792
Author manuscript: the content is identical to the content of the published paper, but without the final typesetting by the publisher

1. Introduction

Aerodynamic drag is responsible for 90% of the total resistance experienced by a cyclist at racing speeds (± 60 km/h in team pursuit) [1]. It is mainly related to the position of the cyclist on his bicycle, but also inherently to his anthropometric characteristics (body dimensions), further referred to as his stature. Previous research by field testing and wind-tunnel experiments [2-6] showed that even minor adjustments to a cyclist's position can result in a decrease of the aerodynamic drag. Many elite cyclists therefore try to optimise their position for drag by means of field tests or wind-tunnel tests [7]. However, improving the position from an aerodynamic point of view does not necessarily result in optimised metabolic cost and respiratory functions. In terms of race performance, the optimal position is, therefore, often considered to be a compromise between power output and aerodynamics.

In team pursuit (four cyclists for men, three for women), additional complexity is present as drag optimisation of each individual cyclist does not necessarily lead to the lowest drag for the entire group. Furthermore, the drag experienced by a cyclist also depends on the position in the pace line in which they ride. The leader will experience the largest drag, compared to all other positions in the pace line, and provides shelter to the others. Note that the leader of a sequence in team pursuit swings up the track after some time and joins at the end of the group, which leads to a new sequence of riders, so periodical switching occurs. In addition, due to the different stature and position on the bicycle of each cyclist, the total drag of the group will also depend on the specific sequence of the cyclists in the pace line.

Previous experimental research on the effect of drafting, i.e., aerodynamic interference between cyclists, was performed on a tandem of cyclists [1, 8-11], but also on four (or more) cyclists riding in a pace line [2, 9, 12-14]. The second and subsequent cyclists were found to benefit significantly from drafting. The influence of stature, as well as position on the bicycle, on the drafting effect was investigated by Edwards and Byrnes [8] by considering different cyclists. They found that the leader's stature had a large influence on the drafting effect, and that a large variability on the drafting effect was present between different drafters, indicating a strong interaction between leader and drafter. For a four-cyclist pace line (i.e., team pursuit), all experiments, except the ones of Broker [2], were performed in the field, because simultaneous drag measurements of each individual cyclist in a pace line are not straightforward in most wind tunnels.

In these field or wind-tunnel tests, the aerodynamic improvements typically are obtained by trial-and-error since usually only information on the overall cyclist drag is available. Rarely, these improvements are analysed more in detail by

considering the resulting changes in the flow field, since flow-field measurements are often time-consuming and are quite difficult to set up for field tests. An alternative technique is computational fluid dynamics (CFD), which has already been applied for drag evaluation in cycling [15-21] and in other sport disciplines [22-27]. CFD has not been used, to the knowledge of the authors, to evaluate aerodynamic drag for team pursuit, thus for multiple cyclists riding in a pace line. The main advantage of CFD for this particular application is that drag information is available at a high spatial resolution, i.e., for each individual cyclist, including different body segments, together with flow-field information around the cyclists, which can increase insight in drag reduction mechanisms.

In this study, CFD will be used to evaluate the aerodynamic drag of four cyclists riding in a pace line. Each cyclist is different with respect to stature and position on the bicycle. Four different sequences will be evaluated, namely for each cyclist riding in first position. In addition, each sequence will be evaluated for two arm spacings, i.e., lower arms spaced close together and spaced wide. Following issues will be addressed: (i) The drag of an individual cyclist will be compared with his drag in each position in the pace line to evaluate the drag reduction by riding in a pace line; (ii) The total drag of the group will be compared for four different sequences to evaluate which sequence results in the lowest drag; (iii) Two arm spacings will be compared to see if riding with a wider arm spacing, which is not beneficial for an individual cyclist, could, contra-intuitively, lead to a drag decrease of the entire group, as the leader creates a larger wake zone for the drafting cyclists.

2. Materials and methods

2.1 Numerical model

Four male cyclists of the Belgian Track Cycling Team were used as models for the CFD analysis, in time-trial position. The work was approved by the appropriate ethical committees related to the institution in which it was performed and the participants gave informed consent to the work. A digital model of each cyclist was obtained using a high-resolution 3D laser scanning system (K-Scan, Nikon Metrology, Belgium), capturing his specific anthropometric characteristics and his unique position on the bicycle (Figure 1), and was used for computational modelling. For meshing purposes, surface details were smoothed out to some extent. The bicycles were not included in the computational model since this was necessary to limit its complexity: with the bicycles, a too high degree of detail of the computational mesh would be

required since they consist of very small and slender parts. The grids are hybrid grids, consisting of prismatic cells in the boundary-layer region on the cyclist's surface, tetrahedral elements in the vicinity of the cyclist and hexahedral elements further away from the cyclist, which resulted in a total amount of 7.6-7.9 x 10^6 computational cells for computational domains with individual cyclists, and of 21.1-21.2 x 10^6 computational cells for pace lines of four cyclists with normal and wide arm spacings, respectively. The grids were built according to best practice guidelines in CFD [28], based on a grid sensitivity analysis on multiple grids. More detailed information on the grids used, and the discretisation can be found in Defraeye et al. [16-17] and Blocken et al. [15]. The average cell size in the wake region is about 0.03 m. The y^+ values on the surfaces of the cyclists were below 3, indicating a high grid resolution in the boundary-layer region, which is required for low-Reynolds number modelling (LRNM).

The position of the cyclists is similar, apart from the leg position of cyclist 2, which is reversed (i.e., left foot is positioned more upstream than right foot). Each cyclist model was divided into 23 body segments (Figure 2), which were similar (i.e., approximately of the same size and located on the same position on the body) for all cyclists to allow mutual comparison. Four pace-line sequences were evaluated (Figure 3), where it was assumed that the leader of a sequence swings up the track and joins at the end of the group for the next sequence, to mimic the periodical switching during the race. Each sequence was evaluated for two lower arm spacings (Figure 4), namely for a normal (i.e., original, preferred arm position for each rider) and a wider position of the lower arm. The drag of the individual cyclists (normal arm spacing) was also evaluated for comparison purposes. The order of the cyclists making up the pace line was based on the current order in that cycling team. Note that other orders of cyclists in the pace line are also possible, but were not evaluated in the present study.

The virtual cyclists were placed in a particular pace-line sequence in a computational domain, representing the surrounding environment, with the wind direction parallel to the bicycle axis. This domain is presented in Figure 5 for a single cyclist. For a sequence of four cyclists, the computational domain is similar, but longer since the same downstream distance was used (16.7 m). The distance between the cyclists was determined assuming that the distance between their bicycles is quasi zero. At the inlet, a low-turbulent, uniform free-stream flow was imposed with an approach-flow air speed (U_∞) of 60 km/h (16.7 m/s), which is a typical racing speed, and a turbulence intensity of 0.02%. The cyclist's surface was modelled as a no-slip boundary (i.e. a wall) with zero roughness. For the lateral (side) surfaces of the computational domain, a slip-wall boundary (symmetry) was used. Slip walls assume that the normal

velocity component and the normal gradients at the boundary are zero, resulting in flow parallel to the boundary. At the outlet of the computational domain, an ambient static pressure was imposed. The maximal blockage ratio was below 1%, which is well below the recommended value of 3% [29-30].

Note that the approach-flow conditions in this study (i.e., low turbulence intensity and a uniform velocity profile), as applied in most wind-tunnel experiments on cyclist aerodynamics, are representative for the case where only the cyclists are moving and where the air speed of the surrounding air is zero. This situation is representative for that found in indoor environments (e.g., a velodrome), as here air speeds are relatively low. Although they are often not equal to zero, e.g., due to natural convective flow or since cyclists themselves induce air flow in a velodrome, these air speeds can be considered negligible compared to the speed of the cyclists.

2.2 Numerical simulation

When using CFD, detailed validation with experiments is strongly advised to quantify the accuracy of the applied CFD modelling techniques for the specific flow problem. Recently, Defraeye et al. [16-17] performed detailed wind-tunnel measurements on a cyclist (full-scale and scale model) where, apart from drag, also surface pressures were measured on several locations (up to 115) on the cyclist's body. Detailed data sets were obtained, which were used for CFD validation. They found that with steady Reynolds-averaged Navier-Stokes (RANS), which is much less computationally expensive than large-eddy simulation, sufficiently accurate drag and surface pressure predictions could be obtained. The RANS shear-stress transport k-ω turbulence model showed the best overall performance but also the standard k-ε model [31] performed well, if combined with low-Reynolds number modelling (LRNM) to resolve the boundary layer on the cyclist's surface. This k-ε model showed differences with experiments of 11% (full-scale; [16]) and below 5% (scale model; [17]) for drag. For computational stability reasons, related to the large size of the computational domain, the standard k-ε model was preferred in the present study over the shear-stress transport k-ω model. Apart from the aforementioned two extensive validation studies on individual cyclists [16-17], the accuracy of this RANS turbulence model, in combination with LRNM, was also evaluated recently for two drafting cyclist by Blocken et al. [15] by comparison with wind-tunnel measurements, which also showed a satisfactory performance of the CFD model.

The simulations were performed with the CFD code ANSYS Fluent 12, which uses the control volume method. Steady RANS was used, namely the standard k-ε turbulence model [31] in combination with LRNM to resolve the boundary

layer on the cyclist's surface, for which the one-equation Wolfshtein model [32] was used. Note that surface roughness values could not be specified since LRNM was used to model the boundary layer. Surface roughness, for example by wearing an aerodynamically-optimised suit, can however have a (positive) effect on the cyclist drag. Second-order discretisation schemes were used throughout. The SIMPLE algorithm was used for pressure-velocity coupling. Pressure interpolation was second order. Convergence was assessed by monitoring carefully the residuals, but also the velocity and turbulent kinetic energy on specific locations in the flow field and surface friction on the surface of the cyclists. The iterations were terminated when all residuals and other monitors showed no further reduction with increasing number of iterations.

3. Results

3.1 Aerodynamic drag of individual cyclists

Aerodynamic drag is usually quantified by defining a dimensionless drag coefficient (C_D) which relates the drag force (F_D, N) to the frontal area of the cyclist (A, m^2) (see Wilson [33]):

$$F_D = AC_D \frac{\rho U_\infty^2}{2} \quad (1)$$

where ρ is the density of air (kg/m^3) and U_∞ is the approach-flow air speed (m/s). Often, the drag area (AC_D) is reported instead of C_D since it does not require an explicit determination of the frontal area. Since the frontal area of all cyclists differed in this study (see Table 1), the drag area is reported instead of the drag coefficient, which is thus directly representative for the drag force experienced by a cyclist. Note that a distinct dependency of AC_D on the Reynolds number was found by Defraeye et al. [18] for cyclists in the time-trial position, but this effect was predominantly present at air speeds above 60 km/h. Furthermore, the reported drag areas are relatively low since they do not include the bicycle, which also account for about 30% of the total drag. The values of the cyclists (without bicycle) agree well with those found by Defraeye et al. [16] from wind-tunnel tests on cyclists: they found a drag area for an athlete in the time-trial position of 0.134 m² (without bicycle).

The drag area of each individual cyclist ($AC_{D,cyclist}$) is given in Table 1. The drag area of cyclist 1 is clearly much larger than that of the other cyclists, which are all very similar. This is not surprising when considering the stature of cyclist 1 in Figure 1 and 3. Furthermore, no correlation is found between frontal area and drag area: the drag areas of cyclists 2-4

are very similar, but their frontal areas differ significantly. In Figure 6, the drag areas of the different body segments, relative to the total drag area of the cyclist ($AC_{D,cyclist}$, see Table 1), are compared for the different cyclists. The largest drag areas are found for the head, the legs and the upper arms since they compose the major part of the frontal area and since they have a relatively large surface area. Note that negative drag areas indicate a negative drag force, i.e., opposed to the wind direction (negative *y*-direction). Following remarks can be made when comparing the different cyclists: (1) Most body segments show a similar drag area for each of the four cyclists; (2) The drag area of the head of cyclist 4 is clearly much lower, as it is held very streamlined to the rest of the body (Figure 1 and 3); (3) A large variation is found for the drag areas of the legs. Note that the drag areas of the legs of cyclist 2 are not directly comparable since the leg position was reversed, and that in reality the leg position will constantly change during cycling. Assessing drag areas of different body segments by means of such charts is thus particularly valuable for the upper part of the body. Compared to the total cyclist drag area obtained from field or wind-tunnel tests, these charts provide more detailed information, and can be very useful for analysis and optimisation of the cyclist's position on the bicycle. The flow field around the individual cyclists is presented in Appendix 1.

3.2 Position of cyclist in the pace line

In Figure 7, the drag area of different cyclists is given as a function of their position in the pace-line sequence for the four sequences presented in Figure 3. In Figure 7a the drag area is given, and in Figure 7b these drag areas are scaled with the drag area of each individual cyclist ($AC_{D,cyclist}$, see Table 1). When cycling in first position, the drag area reduces about 3%, compared to an individual cyclist. This reduction is due to the altered flow field in the wake of the leading cyclist, which affects amongst others the pressure distribution on its back. This effect is discussed in detail by Blocken et al. [15] and was also confirmed here by wind-tunnel experiments. The drag area of each cyclist reduces even more when cycling in second and subsequent positions, to below 60% of his individual drag. This reduction (in position 2-4) is the largest for cyclist 2, as he is positioned behind the "large" cyclist 1 for all sequences, except for sequence 2 when he is in first position himself. As cyclist 2 experiences less drag when drafting, he will have to provide less power to maintain the speed of the group and thus will be able to rest somewhat more than the other cyclists. In Figure 8, the drag area of the cyclists is given for different sequences as a function of their position in the sequence. Also here it is clear that there is always a significant drop in drag area behind cyclist 1, which provides shelter for cyclist 2 in his wake. The flow field around the different sequences is presented in Appendix 1.

3.3 Total drag of different sequences

In Figure 9a, the total drag area of all four cyclists together (i.e., the entire pace line) is given for the four sequences presented in Figure 3, and for both arm spacings. A distinct variation by a few percent can be noticed between the sequences. Sequence 1 and 4, with cyclist 1 in first and second position, respectively, show the lowest total drag area, which is related to the fact that cyclist 1 provides shelter for the rest of the pace line by his larger stature. These sequences are thus more efficient for the entire group during a race.

3.4 Arm spacing

The influence of the arm spacing on the total drag area of the group is shown in Figure 9a for the four sequences presented in Figure 3. In Figure 9b, the total drag area, averaged over all cyclists in a specific position, is given for both arm spacings as a function of the position in the sequence. From both figures, it is clear that a wider arm spacing leads to an increase of the drag area, and should be avoided. Note that the difference seems smaller in Figure 9b since a different scaling is used. In reality, the arm position will be a compromise between aerodynamics and cycling comfort, where a wider position is more beneficial for the latter. Note however that cyclist 1 had a slightly lower drag area for wider arm spacing in positions 1-3 (not shown in figures). A recent wind-tunnel study showed that handlebar height had a larger impact on the cyclist drag than arm spacing [34]. Nevertheless, both wide and narrow arm spacings were found to be optimal here, depending on specific athlete.

4. Discussion

In previous studies (see section 1), the effect of drafting has been quantified by the reduction in drag (area), power output or oxygen consumption. Since a drag reduction does not result in the same reduction in power, as the rolling resistance does not decrease (e.g., [1, 33]), reporting drag reductions is considered more general. Previously reported drag reductions of the second (drafting) cyclist agree with those found in this study: up to 49% [11], about 40% [1], 23% - 57% [8], 38% [9], 26% [20], 34%-39% [2], 16-30% [15]. It is however clear that a large spread is present.

In a configuration with more than two cyclists riding in a pace line, no significant difference (below a few percent in drag coefficient, power output or oxygen consumption) was usually found between the second and subsequent cyclists [13,14, 20]. Broker et al. [12] and Broker [2], however, found larger differences, i.e., even above 5% (in power output). In the present computational study, also clear differences were found (see Figure 8), which are mainly related to the

presence of the much larger cyclist 1. When cyclist 1 is riding in front or in the back, the variation between the drafting cyclists is much smaller.

Kyle [9] argued that the leading cyclist does not benefit from a drafting cyclist. Iniguez-de-la-Torre and Iniguez [20] however performed a study on 2D elliptic shapes, as simplified models of cyclists, and found a drag reduction of the first one of 4%, for a group of four, which is similar to the findings in the present study (~ 3% reduction for leading cyclist). For a group of two cyclists, Blocken et al. [15] found a drag reduction up to 2.5% for the leading cyclist, where such a drag reduction was also confirmed by wind-tunnel experiments.

Apart from aerodynamics, the performance and fitness of each cyclist is very important in team pursuit, as the group has to ride at the same speed during the race. Therefore, the required effort should not necessarily be evenly distributed amongst the cyclists, but should be optimised to obtain the best performance of the group. Hence, the fastest member of the team should ideally: (1) have the largest drag area, to shelter the other members (see also [8]); (2) be positioned in front of the slowest member of the team; (3) be positioned in the least favourable aerodynamic position, e.g., behind a small cyclist. For the present study, cyclist 1 should preferably be the fastest member and cyclist 2 the slowest.

This is the first study, to the best knowledge of the authors, which evaluates aerodynamics for team pursuit with numerical techniques (computational fluid dynamics), instead of wind-tunnel or field tests. A specific advantage of CFD is that a much higher spatial resolution is available of cyclist drag, namely even of different body segments, and of the flow field. This particular feature helps increasing insight in drag reduction mechanisms of individual cyclists in team pursuit, related to their anthropometric characteristics (stature), the position of each cyclist in the pace line and the sequence in which they ride. Such information on aerodynamic drag of each cyclist in team pursuit can be combined with related information on individual cyclist performance to determine the optimal pace-line sequence for team pursuit. The numerical techniques used in the present study (i.e., CFD) provide complementary information to the commonly used experimental techniques, and should be used accordingly.

6. Conclusions

CFD was applied to evaluate aerodynamic drag of four cyclists in team pursuit, each with a different stature and position on the bicycle, where the bicycles were not included in the numerical model. Four different sequences were evaluated, namely for each cyclist riding in first position, and each sequence was evaluated for two arm spacings. Each individual cyclist had a different drag area, also with respect to the different body segments. When riding in a pace line, the drag of a cyclist was clearly dependent on his position in the pace line, where second and subsequent positions experienced a drag reduction up to 40%, compared to an single cyclist. Individual differences in stature and specific position on the bicycle led to an intercyclist variation of this drag reduction at a specific position but also of the total drag of the group for different sequences. A larger drag area was found when riding with a wider arm spacing for all sequences. Such information on intercyclist variation in aerodynamic drag can be combined with information on cyclist performance to determine the optimal order of the cyclists in a pace line for a team pursuit.

Acknowledgements

Thijs Defraeye is a postdoctoral fellow of the Research Foundation – Flanders (FWO) and acknowledges its support. This study was partially funded by the Flemish Government and by the Flemish Cycling Federation. Special thanks go to Jos Smets, Director of Sport of the Belgian Cycling Federation, for his enduring interest and support to integrate innovation in cycling.

References

[1] Kyle, C.R., and Burke, E.R., 1984, "Improving the Racing Bicycle," Mech. Eng., **106**(9), pp. 34-45.

[2] Broker, J.P., 2003, "Cycling Power: Road and Mountain," In: Burke, E.R., editor. High-Tech Cycling: The Science of Riding Faster (pp. 147-174), Colorado: Human Kinetics.

[3] Garcia-Lopez, J., Rodriguez-Marroyo, J.A., Juneau, C.E., Peleteiro, J., Martinez, A.C., and Villa, J.G., 2008, "Reference Values and Improvement of Aerodynamic Drag in Professional Cyclists," J. Sport Sci., **26**(3), pp. 277-286.

[4] Grappe, G., Candau, R., Belli, A., and Rouillon, J.D., 1997, "Aerodynamic Drag in Field Cycling with Special Reference to the Obree's Position," Ergonomics, **40**(12), pp. 1299-1311.

[5] Jeukendrup, A.E., and Martin, J., 2001, "Improving Cycling Performance – How should we spend our Time and Money," Sports Med., **31**(7), pp. 559-569.

[6] Jobson, S.A., Nevill, A.M., Palmer, G.S., Jeukendrup, A.E., Doherty, M., and Atkinson, G., 2007, "The Ecological Validity of Laboratory Cycling: Does Body Size explain the Difference between Laboratory- and Field-based Cycling Performance?," J. Sports Sci.? **25**(1), pp. 3-9.

[7] Atkinson, G., Davison, R., Jeukendrup, A., and Passfield, L., 2003, "Science and Cycling: Current Knowledge and Future Directions for Research," J. Sport Sci., **21**(9), pp. 767-787.

[8] Edwards, A.G., and Byrnes, W.C., 2007, "Aerodynamic Characteristics as Determinants of the Drafting Effect in Cycling," Med. Sci. Sport. Exer., **39**(1), pp. 170-176.

[9] Kyle, C.R., 1979, "Reduction of Wind Resistance and Power Output of Racing Cyclists and Runners travelling in Groups," Ergonomics, **22**(4), pp. 387-397.

[10] Olds, T., 1998, "The mathematics of breaking away and chasing in cycling," Eur. J. Appl. Physiol. O., **77**(6), pp. 492-497.

[11] Zdravkovic, M.M., Ashcroft, M.W., Chisholm, S.J., and Hicks, N., 1996, "Effect of Cyclist's Posture and Vicinity of another Cyclist on Aerodynamic Drag," In: Haake, S.J., editor. The Engineering of Sport (pp. 21-28)? Rotterdam: Balkema.

[12] Broker, J.P., Kyle, C.R., and Burke, E.R., 1999, "Racing Cyclist Power Requirements in the 4000-m Individual and Team Pursuits," Med. Sci. Sport. Exer., **31**(11), pp. 1677-1685.

[13] Hagberg, J.M., and McCole, S.D., 1990, "The Effect of Drafting and Aerodynamic Equipment on the Energy Expenditure during Cycling?" Cycling Sci., **2**(3), pp.19-22.

[14] McCole, S.D., Claney, K., Conte, J.C., Anderson, R., and Hagberg, J.M., 1990, "Energy Expenditure during Bicycling," J. Appl. Physiol. **68**(2), pp. 748-753.

[15] Blocken, B., Defraeye, T., Koninckx, E., Carmeliet, J., and Hespel, P., 2013, "CFD Simulations of the Aerodynamic Drag of Two Drafting Cyclists," Comput. Fluids, **71**, 435-445.

[16] Defraeye, T., Blocken, B., Koninckx, E., Hespel, P., and Carmeliet, J., 2010, "Aerodynamic Study of Different Cyclist Positions: CFD Analysis and Full-scale Wind-Tunnel Tests," J. Biomech., **43**(7), pp. 1262-1268.

[17] Defraeye, T., Blocken, B., Koninckx, E., Hespel, P., and Carmeliet, J., 2010, "Computational Fluid Dynamics Analysis of Cyclist Aerodynamics: Performance of Different Turbulence-Modelling and Boundary-Layer Modelling Approaches," J. Biomech., **43**(12), pp. 2281-2287.

[18] Defraeye, T., Blocken, B., Koninckx, E., Hespel, P., and Carmeliet, J., 2011, "Computational Fluid Dynamics Analysis of Drag and Convective Heat Transfer of Individual Body Segments for Different Cyclist Positions," J. Biomech., **44**(9), 1695-1701.

[19] Hanna, R.K., 2002, "Can CFD make a Performance Difference in Sport?," In: Ujihashi, S., and Haake, S.J., editors, The Engineering of Sport 4 (pp. 17-30), Oxford: Blackwell Science.

[20] Iniguez-de-la-Torre, A., and Iniguez, J., 2009, "Aerodynamics of a Cycling Team in a Time Trial: does the Cyclist at the Front benefit?," Eur. J. Phys., **30**(6), pp. 1365-1369.

[21] Lukes, R.A., Hart, J.H., Chin, S.B., and Haake, S.J., 2004, "The Aerodynamics of Mountain Bicycles: The Role of Computational Fluid Dynamics," In: Hubbard, M., Mehta, R.D., and Pallis, J.M., editors. The Engineering of Sport 5 (pp. 104-110), Sheffield: International Sports Engineering Association.

[22] Dabnichki, P., and Avital, E., 2006, "Influence of the Position of Crew Members on Aerodynamics Performance of a Two-Man Bobsleigh," J. Biomech., **39**(15), pp. 2733-2742.

[23] Lecrivain, G., Slaouti, A., Payton, C., and Kennedy, I., 2008, "Using Reverse Eengineering and Computational Fluid Dynamics to investigate a Lower Arm Amputee Swimmer's Performance," J. Biomech., **41**(13), pp. 2855-2859.

[24] Minetti, A.E., Machtsiras, G., and Masters, J.C., 2009, "The Optimum Finger Spacing in Human Swimming," J. Biomech., **42**, pp. 2188-2190.

[25] Zaïdi, H., Fohanno, S., Taiar, R., and Polidori, G., 2010, "Turbulence Model Choice for the Calculation of Drag Forces when using the CFD Method," J. Biomech., **43**(3), pp. 405-411.

[26] Zaïdi, H., Taiar, R., Fohanno, S., and Polidori, G., 2008, "Analysis of the Effect of Swimmer's Head Position on Swimming Performance using Computational Fluid Dynamics," J. Biomech., **41**(6), pp. 1350-1358.

[27] Barber, S., Chin, S.B., and Carré, M.J., 2009, "Sports Ball Aerodynamics: A Numerical Study of the Erratic Motion of Soccer Balls," Comput. Fluids, **38**(6), pp. 1091-1100.

[28] Casey, M, and Wintergerste, T., 2000, "Best Practice Guidelines," ERCOFTAC Special Interest Group on "Quality and Trust in Industrial CFD", ERCOFTAC.

[29] Franke, J., Hellsten, A., Schlünzen, H., and Carissimo, B., 2007, "Best Practice Guideline for the CFD Simulation of Flows in the Urban Environment," Hamburg: COST Action 732: Quality assurance and improvement of microscale meteorological models.

[30] Tominaga, Y., Mochida, A., Yoshie, R., Kataoka, H., Nozu, T., Yoshikawa, M., and Shirasawa, T., 2008, "AIJ Guidelines for Practical Applications of CFD to Pedestrian Wind Environment around Buildings," J. Wind Eng. Ind. Aerod., **96**(10–11), pp. 1749-1761.

[31] Jones, W.P., and Launder, B.E., 1972, "The Prediction of Laminarization with a Two-Equation Model of Turbulence," Int. J. Heat Mass Tran., **15**, pp. 301-314.

[32] Wolfshtein, M., , 1969, "The Velocity and Temperature Distribution in One-Dimensional Flow with Turbulence Augmentation and Pressure Gradient," Int. J. Heat Mass Tran., **12**(3), pp. 301-318.

[33] Wilson, D.G.., 2004, "Bicycling Science," USA: MIT Press.

[34] Underwood, L., and Jermy, M., 2013, "Optimal Handlebar Position for Track Cyclists," Sports Eng., **16**(2), pp. 81-90.

Table captions

Table 1. Frontal area (calculated from virtual cyclist models, obtained from scanning), body surface area and drag area of individual cyclists.

Figure captions

Figure 1. Virtual models of four different cyclists, obtained from laser scanning (frontal areas are given in Table 1).

Figure 2. Different body segments of the cyclist: (a) front view; (b) side view.

Figure 3. Different sequences for cyclists riding in a pace line (cyclist is indicated by C).

Figure 4. Two different lower arm spacings for cyclists riding in a pace line for sequence 1 (left: normal, right: wide).

Figure 5. Computational domain for a single cyclist and boundary conditions.

Figure 6. Percentage of drag area for the different body segments ($AC_{D,segment}/AC_{D,cyclist}$) for different individual cyclists at U_∞ = 60 km/h. The total drag area of each cyclist ($AC_{D,cyclist}$) is presented in Table 1.

Figure 7. Drag area of different cyclists as a function of their position in the sequence (for the four sequences presented in Figure 3). Position 0 indicates the drag area of an individual cyclist (see Table 1). (a) drag area; (b) drag area, scaled with the drag area of each individual cyclist (from Table 1).

Figure 8. Drag area of cyclists in different sequences as a function of their position in the sequence. The position of cyclist 1 is indicated by C1.

Figure 9. (a) Total drag area of all cyclists in the pace line for different sequences, for two lower arm spacings;

(b) Average drag area of all cyclists at different positions in a sequence, for two lower arm spacings.

Defraeye T., Blocken B., Koninckx E., Hespel P., Verboven P., Nicolai B., Carmeliet J. (2014), Cyclist drag in team pursuit: influence of cyclist sequence, stature and arm spacing, *Journal of Biomechanical Engineering* 136 (1), 011005. http://dx.doi.org/10.1115/1.4025792
Author manuscript: the content is identical to the content of the published paper, but without the final typesetting by the publisher

Tables

Table 1. Frontal area (calculated from virtual cyclist models, obtained from scanning), body surface area and drag area of individual cyclists.

Cyclist name	Frontal area (m^2)	Surface area (m^2)	Drag area (m^2)
Cyclist 1	0.342	2.17	0.181
Cyclist 2	0.278	1.92	0.145
Cyclist 3	0.295	1.91	0.145
Cyclist 4	0.308	2.05	0.148

Defraeye T., Blocken B., Koninckx E., Hespel P., Verboven P., Nicolai B., Carmeliet J. (2014), Cyclist drag in team pursuit: influence of cyclist sequence, stature and arm spacing, *Journal of Biomechanical Engineering* 136 (1), 011005. http://dx.doi.org/10.1115/1.4025792
Author manuscript: the content is identical to the content of the published paper, but without the final typesetting by the publisher

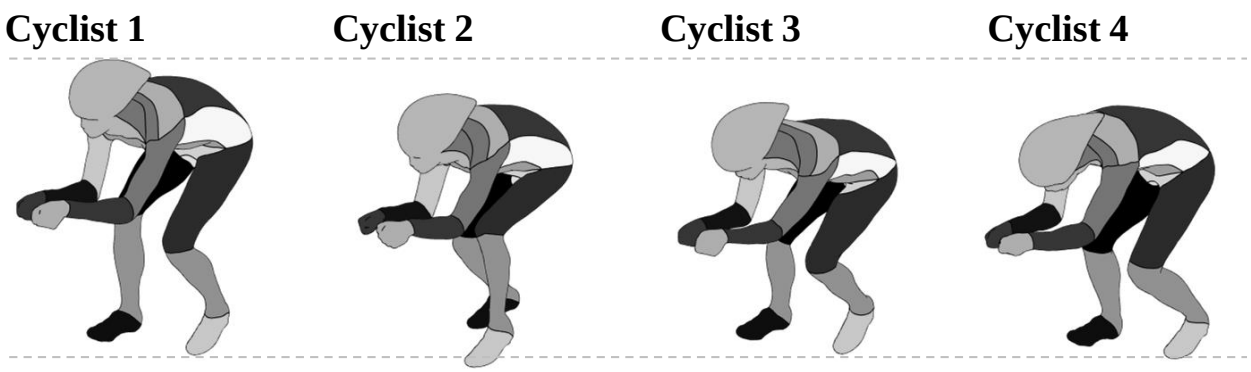

Figure 1. Virtual models of four different cyclists, obtained from laser scanning (frontal areas are given in Table 1).

Defraeye T., Blocken B., Koninckx E., Hespel P., Verboven P., Nicolai B., Carmeliet J. (2014), Cyclist drag in team pursuit: influence of cyclist sequence, stature and arm spacing, *Journal of Biomechanical Engineering* 136 (1), 011005. http://dx.doi.org/10.1115/1.4025792
Author manuscript: the content is identical to the content of the published paper, but without the final typesetting by the publisher

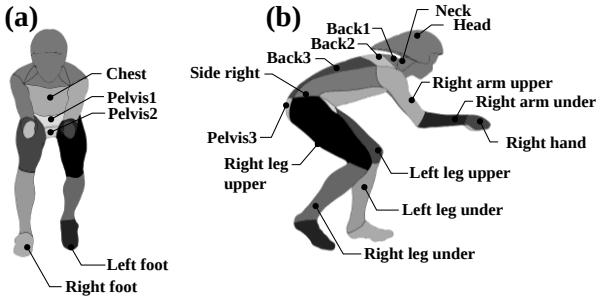

Figure 2. Different body segments of the cyclist: (a) front view; (b) side view.

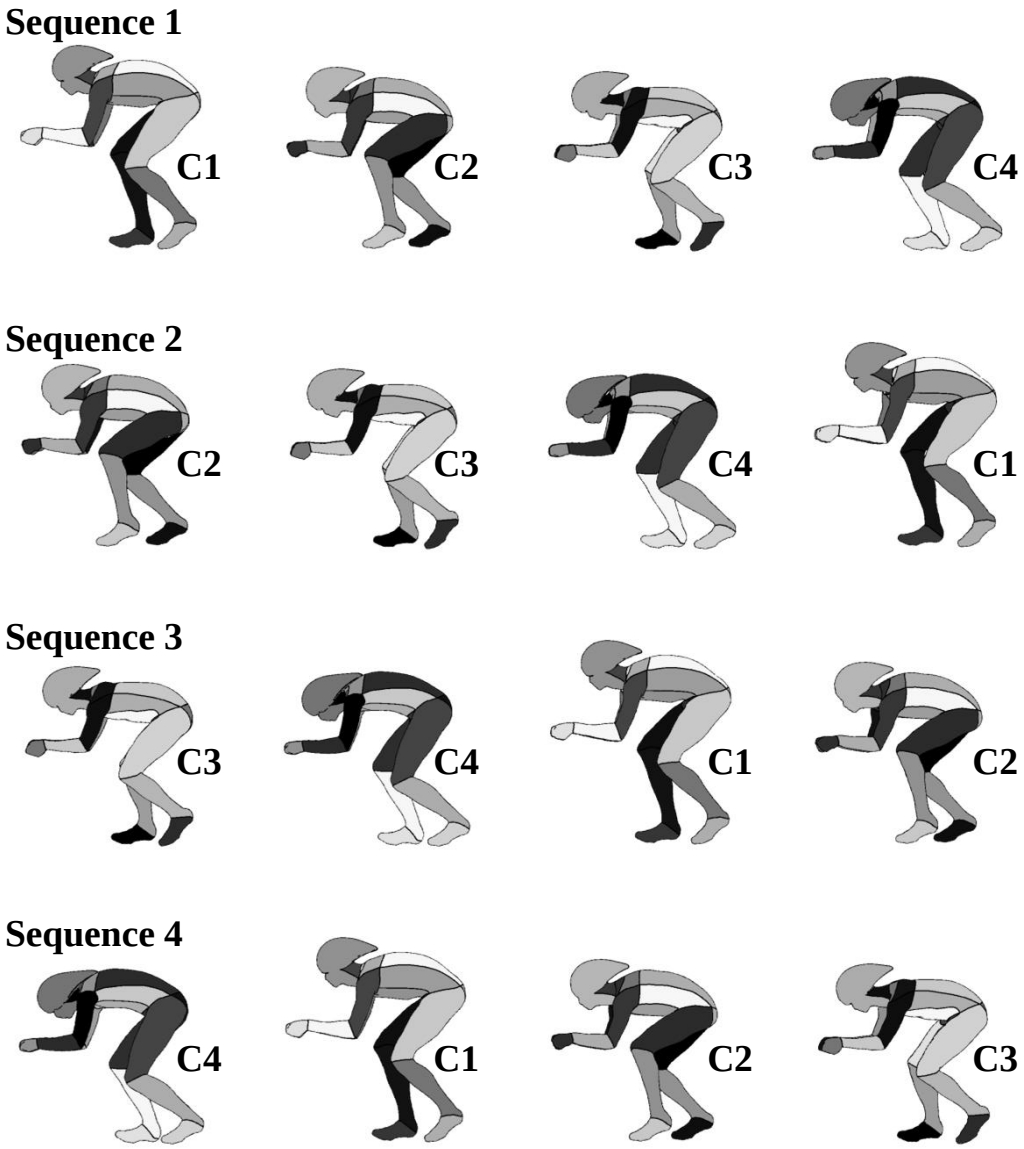

Figure 3. Different sequences for cyclists riding in a pace line (cyclist is indicated by C).

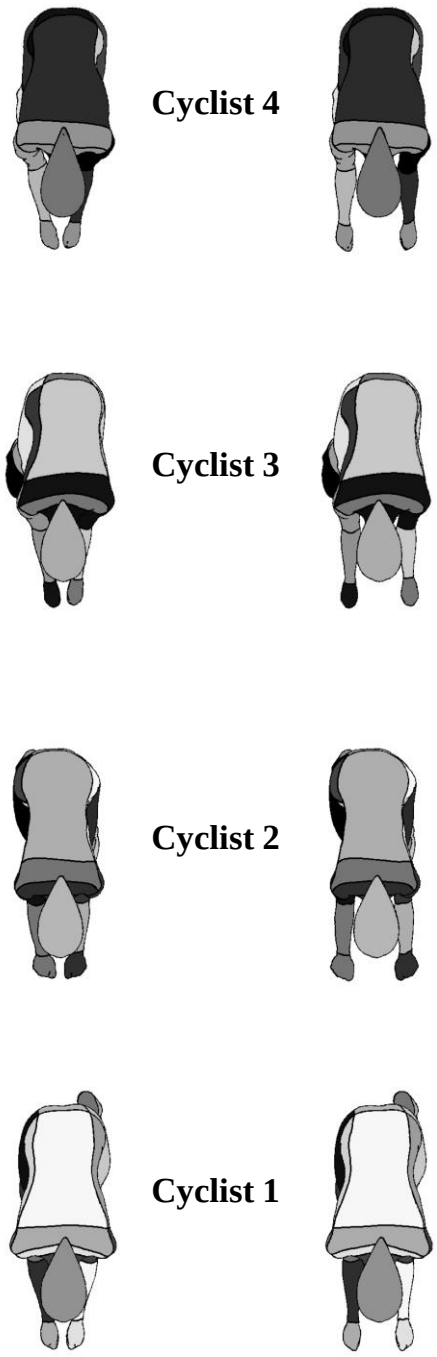

Figure 4. Two different lower arm spacings for cyclists riding in a pace line for sequence 1 (left: normal, right: wide).

Defraeye T., Blocken B., Koninckx E., Hespel P., Verboven P., Nicolai B., Carmeliet J. (2014), Cyclist drag in team pursuit: influence of cyclist sequence, stature and arm spacing, *Journal of Biomechanical Engineering* 136 (1), 011005. http://dx.doi.org/10.1115/1.4025792
Author manuscript: the content is identical to the content of the published paper, but without the final typesetting by the publisher

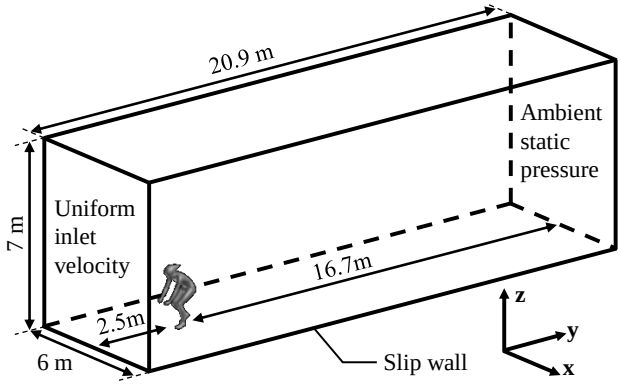

Figure 5. Computational domain for a single cyclist and boundary conditions.

Defraeye T., Blocken B., Koninckx E., Hespel P., Verboven P., Nicolai B., Carmeliet J. (2014), Cyclist drag in team pursuit: influence of cyclist sequence, stature and arm spacing, *Journal of Biomechanical Engineering* 136 (1), 011005. http://dx.doi.org/10.1115/1.4025792
Author manuscript: the content is identical to the content of the published paper, but without the final typesetting by the publisher

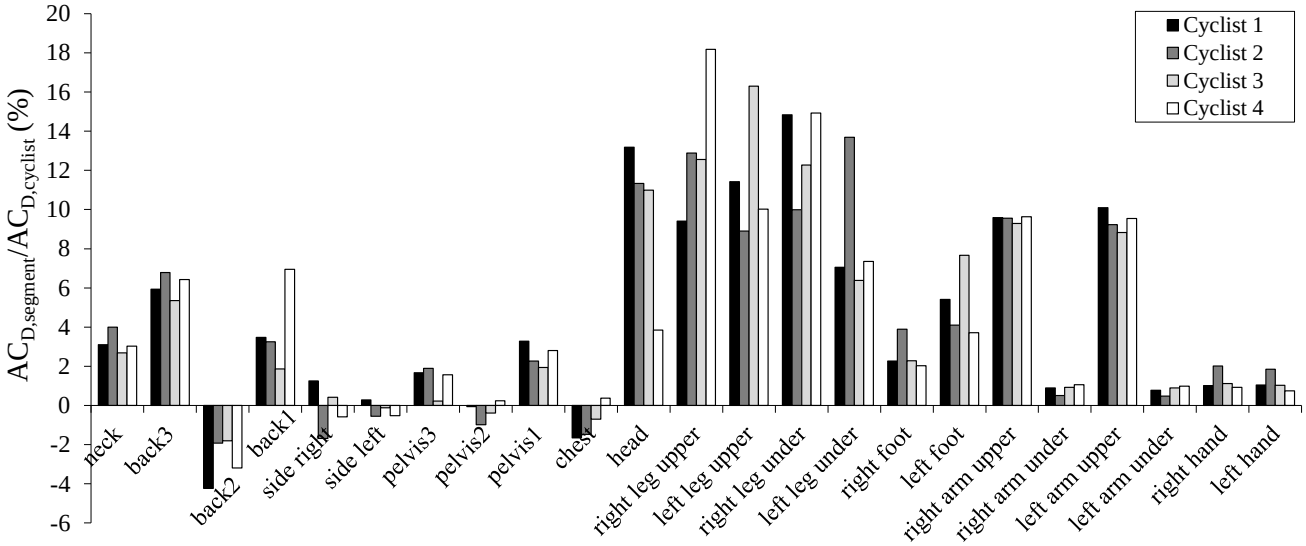

Figure 6. Percentage of drag area for the different body segments ($AC_{D,segment}/AC_{D,cyclist}$) for different individual cyclists at U_∞ = 60 km/h. The total drag area of each cyclist ($AC_{D,cyclist}$) is presented in Table 1.

Defraeye T., Blocken B., Koninckx E., Hespel P., Verboven P., Nicolai B., Carmeliet J. (2014), Cyclist drag in team pursuit: influence of cyclist sequence, stature and arm spacing, *Journal of Biomechanical Engineering* 136 (1), 011005. http://dx.doi.org/10.1115/1.4025792
Author manuscript: the content is identical to the content of the published paper, but without the final typesetting by the publisher

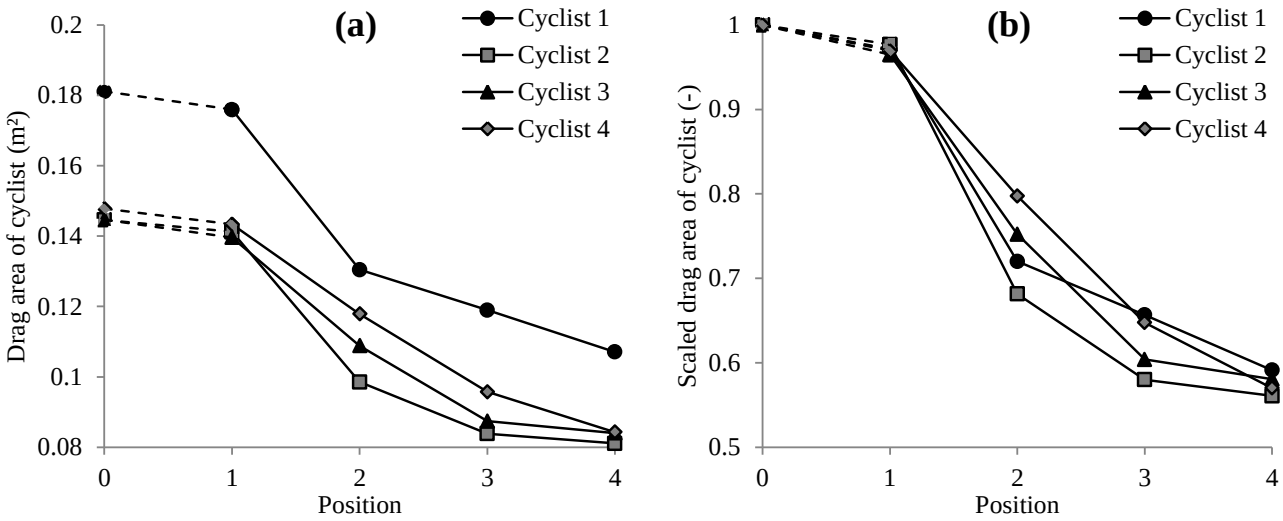

Figure 7. Drag area of different cyclists as a function of their position in the sequence (for the four sequences presented in Figure 3). Position 0 indicates the drag area of an individual cyclist (see Table 1). (a) drag area; (b) drag area, scaled with the drag area of each individual cyclist (from Table 1).

Defraeye T., Blocken B., Koninckx E., Hespel P., Verboven P., Nicolai B., Carmeliet J. (2014), Cyclist drag in team pursuit: influence of cyclist sequence, stature and arm spacing, *Journal of Biomechanical Engineering* 136 (1), 011005. http://dx.doi.org/10.1115/1.4025792
Author manuscript: the content is identical to the content of the published paper, but without the final typesetting by the publisher

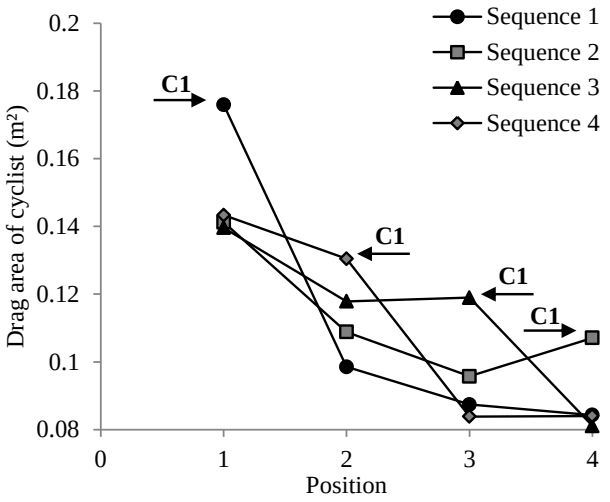

Figure 8. Drag area of cyclists in different sequences as a function of their position in the sequence. The position of cyclist 1 is indicated by C1.

Defraeye T., Blocken B., Koninckx E., Hespel P., Verboven P., Nicolai B., Carmeliet J. (2014), Cyclist drag in team pursuit: influence of cyclist sequence, stature and arm spacing, *Journal of Biomechanical Engineering* 136 (1), 011005. http://dx.doi.org/10.1115/1.4025792
Author manuscript: the content is identical to the content of the published paper, but without the final typesetting by the publisher

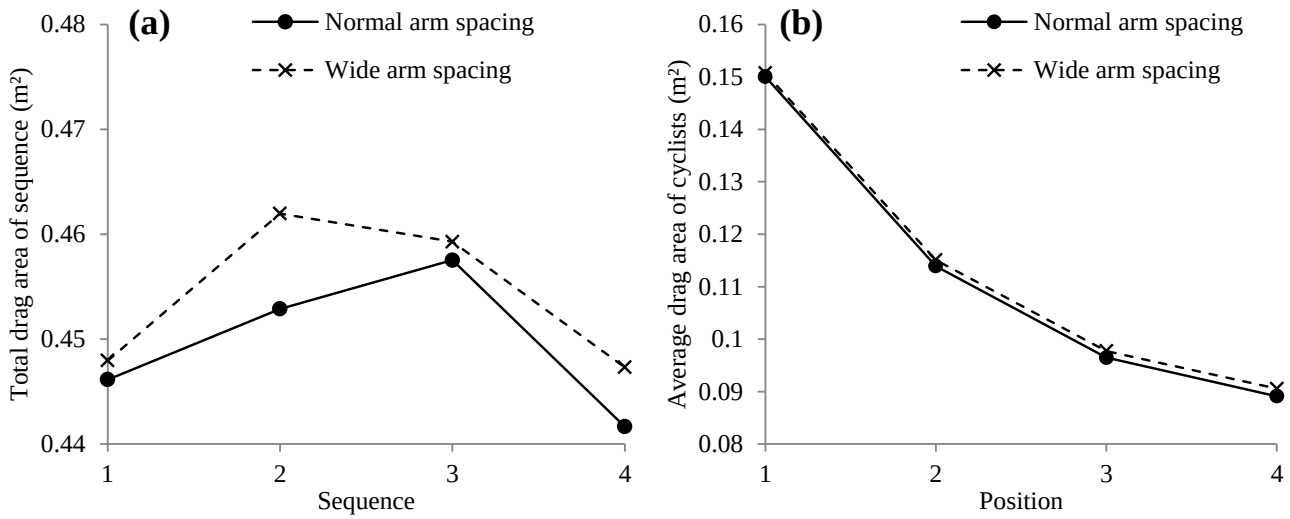

Figure 9. (a) Total drag area of all cyclists in the pace line for different sequences, for two lower arm spacings; (b) Average drag area of all cyclists at different positions in a sequence, for two lower arm spacings.

Defraeye T., Blocken B., Koninckx E., Hespel P., Verboven P., Nicolai B., Carmeliet J. (2014), Cyclist drag in team pursuit: influence of cyclist sequence, stature and arm spacing, *Journal of Biomechanical Engineering* 136 (1), 011005. http://dx.doi.org/10.1115/1.4025792
Author manuscript: the content is identical to the content of the published paper, but without the final typesetting by the publisher

Appendix 1 (Supporting information, intended for online access)

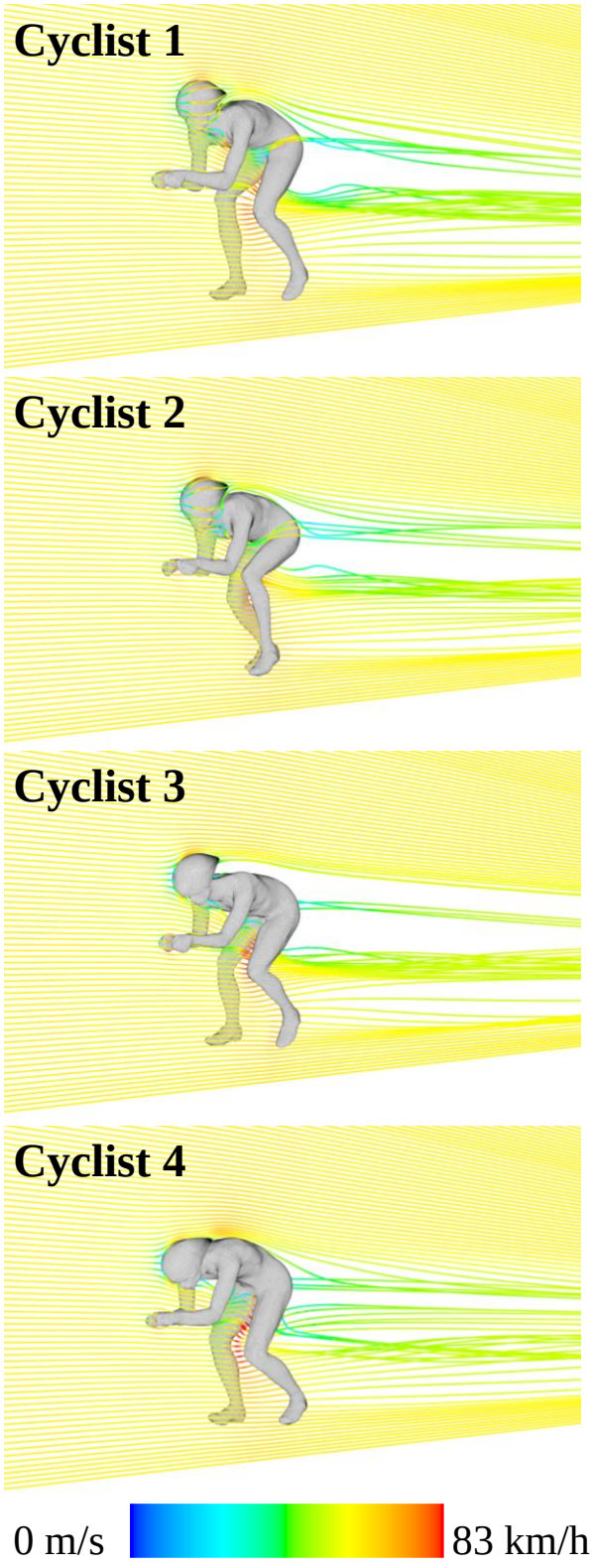

Figure 1 (Appendix). Streamlines, coloured by velocity, for different individual cyclists at U_∞ = 60 km/h.

Defraeye T., Blocken B., Koninckx E., Hespel P., Verboven P., Nicolai B., Carmeliet J. (2014), Cyclist drag in team pursuit: influence of cyclist sequence, stature and arm spacing, *Journal of Biomechanical Engineering* 136 (1), 011005. http://dx.doi.org/10.1115/1.4025792
Author manuscript: the content is identical to the content of the published paper, but without the final typesetting by the publisher

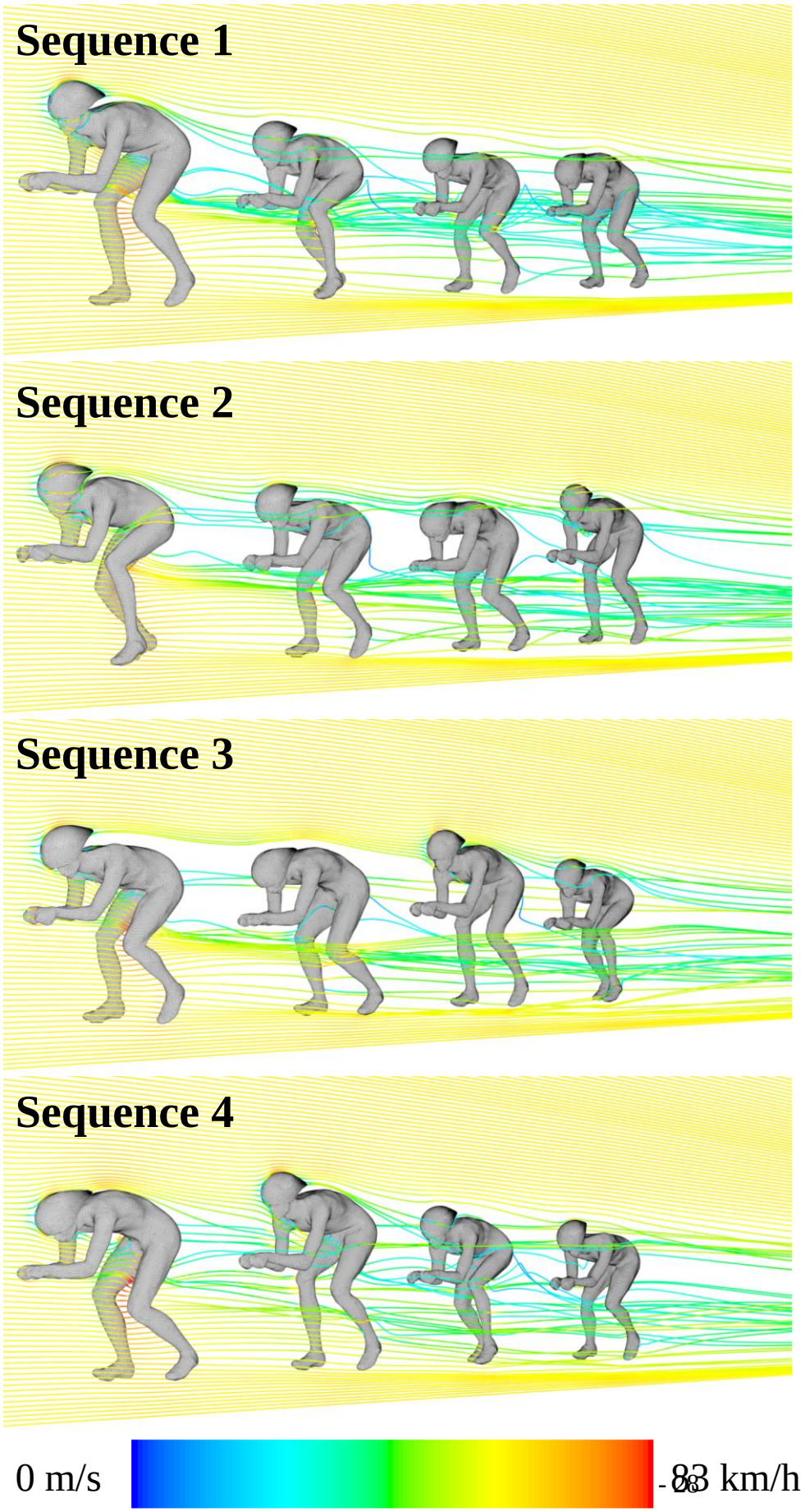

Defraeye T., Blocken B., Koninckx E., Hespel P., Verboven P., Nicolai B., Carmeliet J. (2014), Cyclist drag in team pursuit: influence of cyclist sequence, stature and arm spacing, *Journal of Biomechanical Engineering* 136 (1), 011005. http://dx.doi.org/10.1115/1.4025792
Author manuscript: the content is identical to the content of the published paper, but without the final typesetting by the publisher

Figure 2 (Appendix). Streamlines, coloured by velocity, for four pace-line sequences at U_∞ = 60 km/h.

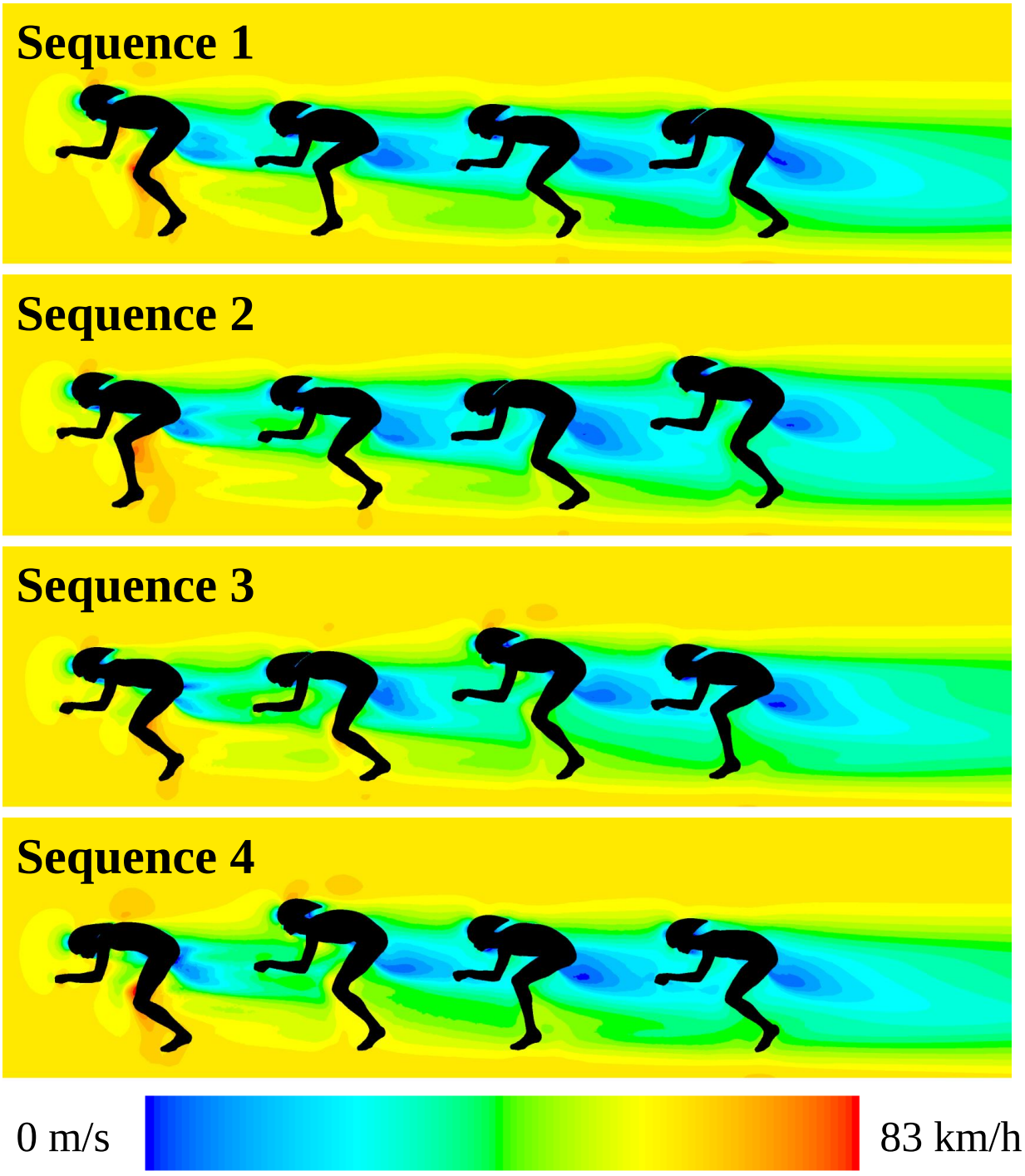

Figure 3 (Appendix). Contours of velocity in a vertical centreplane for four pace-line sequences at U_∞ = 60 km/h.

Defraeye T., Blocken B., Koninckx E., Hespel P., Verboven P., Nicolai B., Carmeliet J. (2014), Cyclist drag in team pursuit: influence of cyclist sequence, stature and arm spacing, *Journal of Biomechanical Engineering* 136 (1), 011005. http://dx.doi.org/10.1115/1.4025792
Author manuscript: the content is identical to the content of the published paper, but without the final typesetting by the publisher